

Design of Space-Filling Antennas for Passive UHF RFID Tags

Benjamin D. Braaten¹, Gregory J. Owen² and Robert M. Nelson³

¹*North Dakota State University*

²*Sebesta Blomberg and Associates*

³*University of Wisconsin – Stout
United States*

1. Introduction

Every year researchers and engineers are finding new and useful applications for Radio Frequency Identification (RFID) systems (Finkenzeller, 2003). Because of the growing use of RFID systems, many different areas of research have also been developed to improve the performance of such systems. A few of these areas of research include novel antenna designs (Rao et al., 2005; Calabrese & Marrocco, 2008; Amin et al. 2009), analysis on the backscatter properties of RFID tags (Yen et al., 2007; Feng et al., 2006), mutual coupling between RFID tags (Li et al., 2008; Owen et al., 2009) and the deployment of RFID systems to complex and extreme environments (Qing & Chen, 2007; Sanford, 2008). There are many aspects to each area of research in RFID. A major topic in many of these areas involves research on the antenna design for RFID tags.

This chapter will focus on the design of efficient space-filling antennas for passive UHF RFID tags. First, an introduction to RFID systems is presented. This is done by describing the major components in a RFID system and how they communicate. Then, the particular backscattering properties of a passive tag are described from a unique electric field integral equation standpoint and from an overall systems perspective (i.e., using the Friis transmission equation). This discussion will then be followed by a section describing a practical design process of various space-filling antennas for passive tags. Finally, a summary of future work and a conclusion about the chapter is presented.

2. An introduction to RFID systems

The two main components of a RFID system are the readers and the tags. An overview of a RFID system is shown in Fig. 1. A reader consists of an antenna, transmitter/receiver and typically an interface with a PC (or other device for viewing information) while a tag has an antenna and an integrated circuit (IC) connected to the antenna (Fig. 2). The reader is a device that transmits electromagnetic energy and timing information into the space around itself to determine if any tags are in the region. This region around the reader is sometimes called the interrogation zone (Finkenzeller, 2003). If a tag is in the interrogation zone (i.e., or interrogated by the reader), the tag will use the IC connected to the antenna to establish communications with the reader and transmit the appropriate information. The max

possible distance that a tag can be interrogated by the reader is referred to as the max read range of the tag.

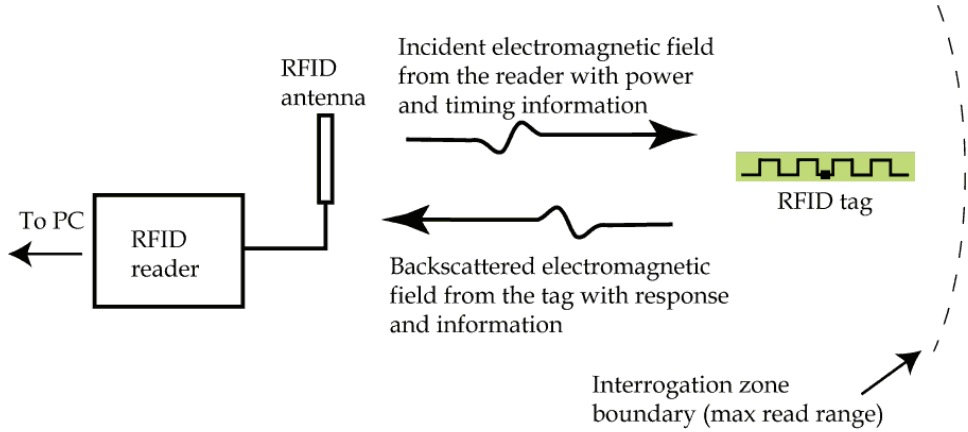


Fig. 1. Overview of a RFID system.

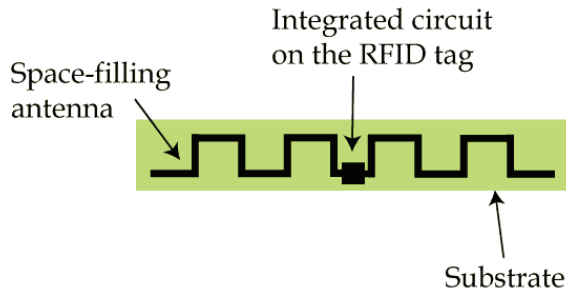


Fig. 2. A Passive RFID tag.

In general, RFID systems can be placed into three major categories: active, semi-passive and passive (Finkenzeller, 2003). An active tag has an onboard battery and can communicate with the reader using only the power from the battery on the tag. A semi-passive tag (or battery assisted tag) is awakened by the incident electromagnetic field from the reader antenna and uses the onboard battery to communicate with the reader. This greatly increases the read range of the tag. Finally, a passive tag does not have an onboard battery. The incoming electromagnetic field from the reader induces a port voltage on the tag antenna while a power harvesting circuit in the IC loads the antenna and uses the port voltage and current to provide power to the digital portion of the IC. This power is then used by the IC to identify itself and communicate back to the reader. An IC on a passive tag is usually referred to as a passive IC. A passive IC communicates with the reader by changing the input impedance of the power harvesting circuit. The impedance is changed between two different values to represent a logic 0 and 1 in a digital signal. Changing this

input impedance results in two different scattered fields from the tag. These scattered fields (backscattered fields) are received by the reader and the digital information is processed. Understanding how these backscattered fields radiate in the region around the RFID tag is important. Because of this and the fact that this chapter focuses on antenna design, the next few sections will present various methods for understanding the backscattered field from the RFID tag.

3. Backscattering properties of a passive RFID tag

Typically, the performance of a RFID system is described using the Friis transmission formula (Rao et al, 2005; Marrocco, 2003). This is a very useful approach to present the performance of a RFID system, and will be done later, but many of the details associated with the tag are not easily extracted from such a presentation. For example, the current distribution on the tag antenna during an interrogation may be of interest or information on the mutual coupling between multiple tags may be a concern. One method to describe other aspects of a passive RFID tag is to derive expressions for the electric field in the region around the tag antenna in terms of the current distribution on the antenna. Once the electric field in the region around the tag is known, many other aspects associated with the RFID tag can be explored. In the following section, the backscattered field from a thin-wire dipole is derived in terms of the load impedance of the antenna. This will show how matching the load impedance with the antenna will result in a much lower scattered field when compared to the case when the terminals are shorted-circuited (Braaten et al., 2006).

3.1 Backscattering from a thin-wire dipole

First, consider the thin-wire dipole shown in Fig. 3 (a) immersed in free-space. E_{inc} represents the incoming wave from the reader and Z_L represents the input impedance of the passive IC. For this discussion, it is assumed that the length L of the antenna is $\lambda/2$ where λ is the wavelength of E_{inc} (i.e., the wavelength of the frequency at which the reader is transmitting at) and that the tag is in the far-field of the reader. This simplifies E_{inc} to a constant value. E_{inc} is travelling in the $-y$ direction and has a \hat{z} - component. As E_{inc} impinges on the thin-wire dipole, a current is induced. This induced current on the thin-wire dipole is assumed to be (Stutzman & Thiele, 1998)

$$I(z) = I_m \sin \left[\beta \left(\frac{L}{2} - |z| \right) \right] \quad (1)$$

where I_m is the maximum current along the antenna, β is the free-space phase constant and $|z| \leq L/2$. This assumption is valid as long as Z_L is chosen in a manner that preserves the sinusoidal current distribution on the thin-wire dipole. One example that would preserve the sinusoidal current distribution would be a 50Ω load connected to a half-wavelength dipole (Braaten et al., 2006). Next, using (1) in the induced emf method, an expression for the open circuit voltage V_{oc} at the port of the dipole can be written in the following manner (Balanis, 2005; Stutzman & Thiele 1998):

$$V_{oc} = -\frac{1}{I(0)} \int_{-L/2}^{L/2} I_m \sin \left[\beta \left(\frac{L}{2} - |z'| \right) \right] E_{inc} dz' \quad (2)$$

where $I(0)$ is the current at the terminals of the dipole. Subsequently, assuming E_{inc} is a constant value and evaluating (2) results in the following expression (Braaten et al., 2006):

$$V_{oc} = -\frac{2E_{inc}}{\beta} \tan\left(\frac{\beta L}{4}\right). \quad (3)$$

Equation (3) is a simple expression for the open circuit voltage of the dipole and it is clear how the incident field from the reader can be used to control the induced voltage.

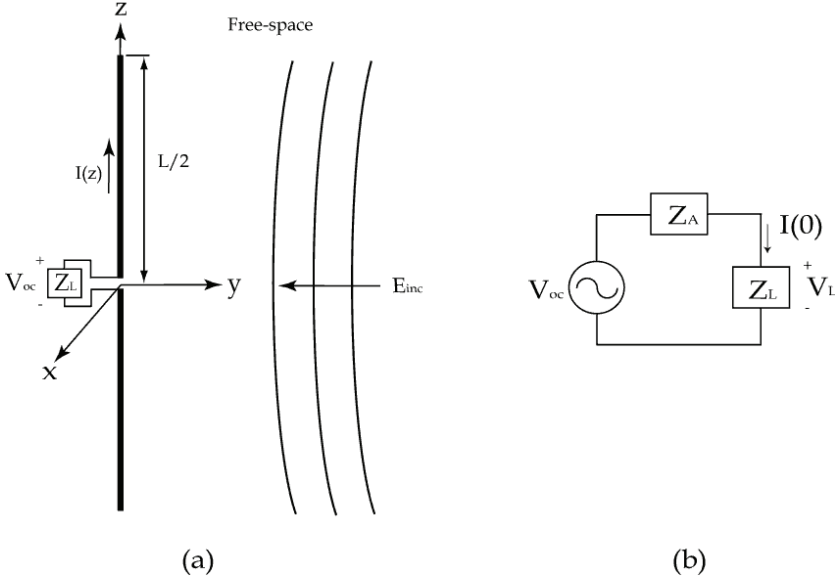


Fig. 3. (a) A thin-wire dipole in free-space; (b) the equivalent circuit of the receiving dipole. Next, consider the equivalent circuit of the receiving dipole shown in Fig. 3 (b) where Z_L and Z_A are the load and antenna impedance values, respectively. Using voltage division, the load voltage can be written as

$$V_L = \frac{Z_L}{Z_L + Z_A} V_{oc} = Z_L I(0). \quad (4)$$

Then, substituting (1) and (3) into (4) and solving for I_m gives:

$$I_m = -\frac{E_{inc}}{(Z_L + Z_A)\beta \cos^2\left(\frac{\beta L}{4}\right)}. \quad (5)$$

Next, an expression for the electric field from the dipole can be written in terms of I_m in the following manner (Balanis, 2005):

$$E_z(\vec{r}) = -j30I_m \left[\frac{e^{-j\beta r_1}}{r_1} + \frac{e^{-j\beta r_2}}{r_2} - \frac{2 \cos(\beta L/2) e^{-j\beta r_0}}{r_0} \right] \quad (6)$$

where $\beta = 2\pi/\lambda$, $r_0 = |\vec{r}|$, $r_1 = |\vec{r}_+ - \vec{r}|$, $r_2 = |\vec{r}_- - \vec{r}|$ and $\vec{r}_\pm = \pm \frac{L}{2} \hat{z}$. Substituting (5) into (6) results in the following expression for the electric field:

$$E_{z,s}(\vec{r}) = \frac{j30E_{inc}}{(Z_L + Z_A)\beta \cos^2\left(\frac{\beta L}{4}\right)} \left[\frac{e^{-j\beta r_1}}{r_1} + \frac{e^{-j\beta r_2}}{r_2} - \frac{2 \cos(\beta L/2) e^{-j\beta r_0}}{r_0} \right]. \quad (7)$$

$E_{z,s}(\vec{r})$ represents the scattered field in the region around the thin-wire dipole as a result of E_{inc} . Equation (7) provides insight as to how the scattered field is closely related to the load impedance. Next, using the notation $E_{inc} = E_{reader}$ and $Z_L = Z_{tag}$, (7) can be written in a more descriptive form:

$$E_{z,s}(\vec{r}) = \frac{j30E_{reader}}{(Z_{tag}+Z_A)\beta \cos^2\left(\frac{\beta L}{4}\right)} \left[\frac{e^{-j\beta r_1}}{r_1} + \frac{e^{-j\beta r_2}}{r_2} - \frac{2 \cos(\beta L/2)e^{-j\beta r_0}}{r_0} \right] \quad (8)$$

where E_{reader} represents the incident field from the reader and Z_{tag} represents the input impedance of the passive IC. From (8), it is clear that by changing Z_{tag} the tag is able to change the scattered field. In an RFID system, this change in scattered field propagates back to the receiving antenna at the reader and the digital information is processed. Noticing how this scattered field is changed by the passive IC is important for successful communication between the reader and the RFID tag.

Next, several load impedances were defined ($Z_{tag} = 0 \Omega, 25 \Omega, 50 \Omega$ and 75Ω) and the resulting scattered field from these different loads were calculated using (8). The scattered field was calculated 1 m from the middle of the dipole in the y-direction with a 1V/m incident field from the reader. The different magnitudes of the scattered fields computed by (8) are shown in Fig. 4. Two characteristics stand out from these computations. First, notice that the largest scattered field is for the short-circuit case. This indicates that more of the energy incident on the dipole is being radiated back into the space around the dipole and not being used by the passive IC. This also improves the chances of the reader picking up the backscattered field from the tag. Second, the lowest scattered field is for the 75Ω load. This is because a 75Ω load has the closest match with the input impedance of the antenna. This also indicates that less energy is being scattered into the region around the dipole and more of it is being used by the load.

The results in Fig. 4 directly show how the field in the region around the dipole can be changed by using different loads at the port of the dipole. Equation (8) could also be used to study the mutual coupling between RFID tags. This coupling information may be important for applications that require many RFID tags to be located in close proximity to one another. In the next section, the far-field characteristics of a RFID system are presented using the Friis transmission equation (Stutzman & Thiele, 1998). This will provide insight as to what characteristics of an RFID tag determine the max read range.

3.2 Describing the wireless RFID system using the Friis transmission equation

The RFID system described in Fig. 1 essentially consists of two transceivers (the reader and passive RFID tag). This type of communication system can be described using the Friis transmission equation (Stutzman & Thiele, 1998):

$$P_{tg} = P_{rd} \frac{G_{rd}G_{tg}\lambda^2}{(4\pi R)^2} q \quad (9)$$

where P_{rd} is the power transmitted by the reader, P_{tg} is the power received by the passive tag, G_{rd} is the gain of the transmitting antenna on the reader, G_{tg} is the gain of the space-filling antenna on the tag, λ is the free-space wavelength of the transmitting frequency by the reader, R is the distance between the antenna on the reader and the antenna on the tag and q is the impedance mismatch factor ($0 \leq q \leq 1$) between the passive IC and the antenna on the tag.

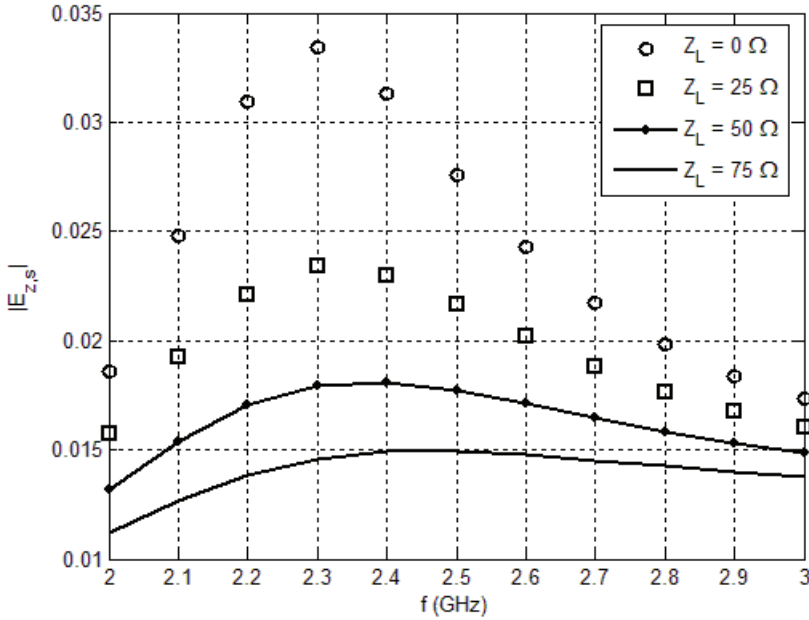


Fig. 4. Backscattered field as a result of changing the load impedance ($L = 6\text{cm}$, $a = 1\text{mm}$).

Equation (9) assumes a polarization match between the antenna used by the reader and the antenna on the tag and that the tag is in the far-field of the reader. Several comments can be made about (9). First, the power at the tag depends very much on G_{tg} (the gain of the space-filling antenna on the RFID tag). A larger gain would mean more power for the passive IC on the tag. Second, using a longer wavelength would improve the power at the tag. Third, a good match between the passive IC and antenna is essential for improving power delivery to the passive IC on the tag. Fourth, the power available to the tag reduces by the distance squared as the tag and reader antenna are moved apart.

An alternate expression for (9) can also be derived. Solving for R in (9) results in the following expression (Braaten et al., 2008; Rao et al., 2005):

$$R = \frac{\lambda}{4\pi} \sqrt{\frac{qG_{rd}G_{tg}P_{rd}}{P_{tg}}}. \quad (10)$$

Next, if the threshold power required to activate the passive IC and communicate with the reader is denoted as P_{th} , then a maximum read range r_{max} can be derived from (10) with a small substitution:

$$r_{max} = \frac{\lambda}{4\pi} \sqrt{\frac{qG_{rd}G_{tg}P_{rd}}{P_{th}}}. \quad (11)$$

Equation (11) is a very useful expression for predicting the max read range of a passive RFID tag. Normally, P_{th} of the passive IC used on the tag is known while P_{rd} and G_{rd} are fixed. This leaves the two variables G_{tg} and q available for a designer. Typically, a tag is

designed to make the most of r_{max} . One method of maximizing r_{max} is to design a tag with a good value of q and a sizeable G_{tg} .

In summary, (11) effectively shows which antenna properties on the RFID tag will determine the max read range of the tag. In the next section, the concept of effective apertures is presented and the maximum power available for the passive IC on the RFID tag is discussed. It will be shown that even with a perfect conjugate match (i.e., $q = 1$) between the antenna on the RFID tag and the input impedance of the passive IC, only half of the available power incident on the tag will be available to the passive IC. The other half of the power is scattered into the region around the tag.

3.3 Effective apertures and power delivery on the RFID tag

Several computations can be carried out to determine the maximum available power from the RFID reader. First, the power density S of the incident wave from the reader has to be considered. From this incident power, the tag has to extract as much power as possible. This extracted power is proportional to S by some factor. This proportionality factor is denoted as the maximum effective aperture A_e and is defined in the following manner (Stutzman & Thiele, 1998):

$$P_{tg} = A_e S \quad (12)$$

where again P_{tg} is the power received by the passive tag. A_e can be derived in terms of the load impedance and S . To derive this expression, first consider the equivalent circuit of the RFID antenna in Fig. 3 (b). The current flowing through the load impedance can be written as:

$$I(0) = \frac{V_{oc}}{Z_L + Z_A} \quad (13)$$

where $Z_L = R_L + jX_L$ and $Z_A = R_A + jX_A$. The real power used by the load resistance is $P_{tg} = I^2(0)R_L$. Next, solving for $I(0)$ in the previous expression and substituting into (13) results in the following expression for P_{tg} :

$$P_{tg} = R_L \left(\frac{V_{oc}}{Z_L + Z_A} \right)^2 \quad (14)$$

Then, assuming $Z_L = Z_A^*$ for max power absorption by the load, (14) reduces to the following:

$$P_{tg} = \frac{V_{oc}^2}{4R_L} \quad (15)$$

Equating (12) to (15) and solving for the effective aperture gives:

$$A_e = \frac{V_{oc}^2}{2R_L S} \quad (16)$$

The effective aperture can also be thought of as the effective area of the antenna. The units for (16) are m^2 , which is also another useful way of thinking about the behavior of an antenna on a RFID tag. By reducing the load resistance, the effective area of the RFID antenna can be improved and hence more power can be delivered to the passive IC.

Also notice that the resistance in the antenna is also absorbing power. This can be seen when considering the equivalent circuit in Fig. 3 (b). Again, assuming $Z_L = Z_A^*$, the power

absorbed by the antenna is the same as the power absorbed by the tag as described in (15). This means that only half of the power delivered to the antenna is absorbed by the passive IC. The rest of the power is scattered into the region around the RFID tag. This scattering loss characteristic is referred to as the scattering aperture A_s of the antenna (Balanis, 2005) and can be calculated using

$$P_A = A_s S \quad (17)$$

where P_A is the power absorbed by the antenna (not the passive IC).

The previous discussion was meant to outline many of the important properties of RFID systems. Several of these concepts will be used in the next sections to design compact space-filling antennas for passive UHF RFID tags with very useful max read range values.

4. Designing space-filling antennas

Space-filling antennas are very useful for designing printed dipoles that resonate in a very small space. Because of these characteristics, space-filling (or meander-line) antennas have been very popular designs for passive RFID tags. It turns out that by using the periodic nature of space-filling antennas, a designer can design compact space-filling antennas with good matching properties and large gains (>2.0 dBi).

4.1 Design of a compact and efficient space-filling antenna

The design process presented here starts with the meander-line antenna shown in Fig. 5 (a) (Braaten et al., 2008). Each dipole arm of the meander-line antenna has N elements. The first step is to determine the electrical length of each dipole arm, which is the sum of the electrical lengths of each meander-line segment in Fig. 5 (b). The electrical length between nodes e_{m-1} and a_m is denoted as L_{e_{m-1},a_m}^e . Similarly, the electrical length between the remaining nodes in Fig. 5 (b) are written as L_{a_m,b_m}^e , L_{b_m,c_m}^e , L_{c_m,d_m}^e and L_{d_m,e_m}^e . Thus, the entire electrical length of the m^{th} segment is $L_m^e = L_{e_{m-1},a_m}^e + L_{a_m,b_m}^e + L_{b_m,c_m}^e + L_{c_m,d_m}^e + L_{d_m,e_m}^e$. Therefore, the total electrical length of each pole is

$$L_p^e = \sum_{n=1}^N L_n^e. \quad (18)$$

Notice the expression in (18) does not have an assumption on the symmetry of each meander-line element in Fig. 5 (b). To simplify the design process, the following symmetry assumptions will be enforced on each meander-line segment: $H_m^e = L_{e_{m-1},a_m}^e = L_{a_m,b_m}^e = L_{c_m,d_m}^e = L_{d_m,e_m}^e$. This then simplifies (18) down to

$$\tilde{L}_p^e = \sum_{n=1}^N H_n^e + L_{b_n,c_n}^e. \quad (19)$$

The next step in the design process is to define the meander-line antenna in Fig. 5 (a) with 2-3 meander-line segments on the dielectric substrate the RFID tag will be attached to. Then, add (or subtract) meander-line elements symmetrically to each dipole arm until a maximum gain is reached. This process can easily be performed in many different numerical electromagnetics software. Once the desired gain is achieved, several pivot points need to be defined on the meander-line antenna. Then, each pole of the meander-line antenna is moved around these pivot points to reduce the overall size of the antenna. This movement is shown in Fig. 6. This reduces the very long meander-line antenna down to a much smaller space-

filling antenna. It has been noticed that significant gains can still be achieved by pivoting the meander-line antenna in this manner. Once the antenna fits into the desired space, an inductive loop may need to be added to conjugate match the input impedance of the antenna with the input impedance of the passive IC.

4.2 Design examples

To illustrate the design process, a space-filling antenna was designed for a passive tag on a single dielectric substrate and a passive tag with a dielectric superstrate. The space-filling antenna was modeled in Momentum (Agilent Technologies, 2009).

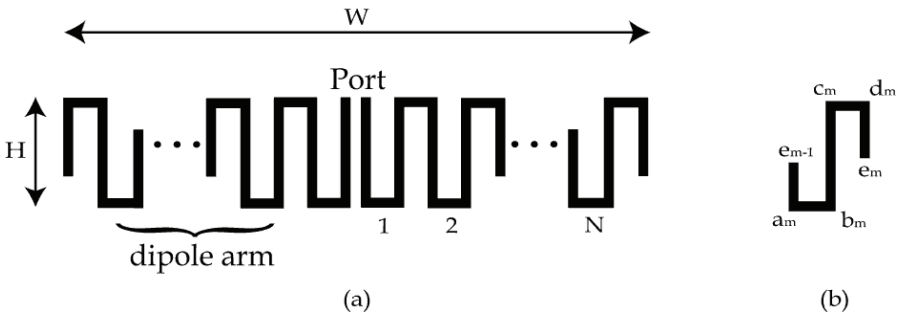


Fig. 5. (a) Meander-line antenna with N -elements on each arm; (b) the m^{th} meander-line element.

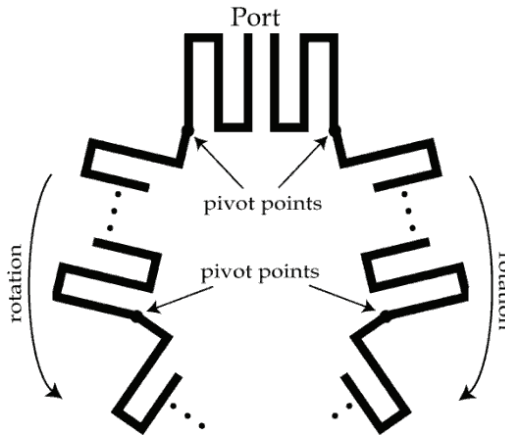


Fig. 6. Rotation of the meander-line antenna into a compact space-filling antenna.

4.3 Space-filling antenna on a single dielectric substrate

As described in the previous section, the first step was to define the size of each meander-line section. For this example, $H_m^e = L_{e_{m-1},a_m}^e = L_{a_m,b_m}^e = L_{c_m,d_m}^e = L_{d_m,e_m}^e = 5$ mm, $L_{b_m,c_m}^e = 10$ mm and the trace width was 1 mm. The substrate had a thickness of $d_1 = 1.58$ mm, permittivity of $\epsilon_1 = 2.2$ and was lossless. The center frequency was 920 MHz. Next, each

meander-line section was connected in series to form a dipole. Meander-line sections were added until a max gain of 4.6 dBi was observed. This resulted in the design shown in Fig. 7 with $N = 13$ on each dipole arm. The input impedance of the meander-line antenna at 920 MHz was $Z_{in} = 9.455 + j23.967 \Omega$. Next, several pivot points were defined along each dipole arm of the meander-line antenna and an inductive matching loop was defined at the port of the antenna. The space-filling antenna in Fig. 8 was a result of this next step. The gain of the space-filling antenna was 2.0 dBi and the input impedance at 920 MHz was $Z_{in} = 32.9 + j168 \Omega$, which matches well with the input impedance of a passive IC (Rao et al., 2005).



Fig. 7. Meander-line antenna on a single substrate ($\epsilon_1 = 2.2$, $d_1 = 1.58$ mm, $G = 4.6$ dBi, $W = 263.8$ mm and $H = 11$ mm).

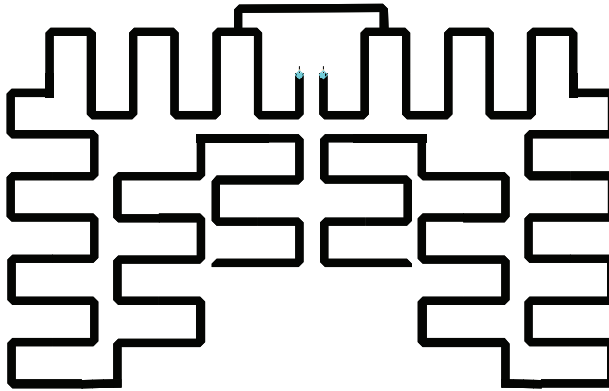


Fig. 8. Space-filling antenna on a single substrate ($\epsilon_1 = 2.2$, $d_1 = 1.58$ mm, $G = 2.0$ dBi, $W = 73$ mm and $H = 46.1$ mm).

4.4 Space-filling antenna with a single dielectric superstrate

Next, a lossless superstrate with a thickness of $d_2 = 1.58$ mm and a permittivity of $\epsilon_2 = 2.2$ (the substrate properties were the same as in the previous example, $d_1 = 1.58$ mm and $\epsilon_1 = 2.2$) was defined above the meander-line antenna. The meander-line sections used in the previous subsection were used in the meander-line design with the superstrate. Meander-line sections were added until a max gain of 4.81 dBi was observed. This resulted in the design shown in Fig. 9 with $N = 12$ on each dipole arm (a similar value of N can be found in the examples presented by Braaten et al, (2008)). The input impedance of the meander-line antenna at 920 MHz was $Z_{in} = 8.256 - j2.281 \Omega$. Just as in the previous section, several pivot points were defined along each dipole arm of the meander-line antenna and an inductive matching loop was defined at the port of the antenna. The space-filling antenna in Fig. 10 was a result of these steps. The gain of the space-filling antenna was 2.0 dBi and the input impedance at 920 MHz was $Z_{in} = 26.080 + j178.592 \Omega$. The antenna in Fig. 10 shows that with proper design, a space-filling antenna with a superstrate can have the same properties as a space-filling antenna without a superstrate.



Fig. 9. Meander-line antenna on a single substrate ($\epsilon_1 = 2.2$, $d_1 = 1.58$ mm, $\epsilon_2 = 2.2$, $d_2 = 1.58$ mm, $G = 4.81$ dBi, $W = 243.8$ mm and $H = 11$ mm).

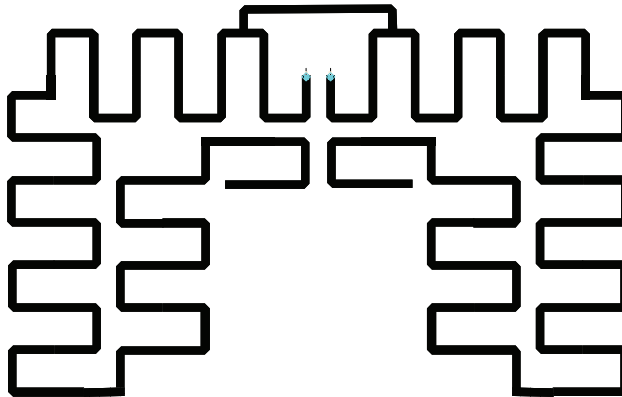


Fig. 10. Meander-line antenna on a single substrate ($\epsilon_1 = 2.2$, $d_1 = 1.58$ mm, $\epsilon_2 = 2.2$, $d_2 = 1.58$ mm, $G = 2.0$ dBi, $W = 73$ mm and $H = 46.1$ mm).

4.5 Other space-filling antenna designs

Finally, it should be mentioned that space-filling antenna designs can be found in other work (Braaten et al., 2008). These designs involve a meander-line antenna on a substrate with a permittivity of 4.25 and a superstrate with a permittivity of 4.0. Several different designs are presented with various meander-line sections and trace widths. The passive RFID prototype tag presented by Braaten et al. (2008) had a max read range of 3.2 m. This was accomplished using the space-filling design techniques presented in the paper and the steps described in the subsections of this chapter. Also, several metamaterial-based (Eleftheriades & Balmain, 2005) designs have been published (Braaten et al., 2009). These designs use metamaterial-inspired elements to reduce the overall size of a space-filling antenna on a passive RFID tag.

5. Future work

A new and rapidly emerging field is the study of metamaterials (Eleftheriades & Balmain, 2005; Marques et al. 2008) to improve the performance of printed antennas, filters, lenses and shielding. Initial studies have shown that the overall size of printed antennas can be reduced while preserving many of the properties of a much larger printed antenna (Lee et al. 2005; Lee et al., 2006; Mirza et al., 2008; Ziolkowski & Lin, 2008). One of the drawbacks of such metamaterial-based antennas is the complicated ground structures, vias and materials needed to reduce the overall size of the antenna. In many instances, these structures are much too complex for use on a passive RFID tag. One possibility that may avoid the need

for complex structures is to use coplanar waveguide structures (CPW). These structures are usually printed on a single conducting plane with an ungrounded substrate. Some researchers have successfully applied metamaterial ideas to achieve much smaller CPW filters (Mao et al., 2007). It is anticipated, that these same principles could be extended to the use of planar antennas on passive UHF RFID tags. In particular, these ideas may be applicable for reducing the space-filling antennas presented in this chapter.

6. Conclusion

In this chapter, an introduction to RFID systems has been presented. The major components of a RFID system were defined and the role of each one was discussed. Then, the characteristics of a RFID system were described using electric field integral equations, the Friis transmission equation and effective apertures. The electric field integral equations showed how the backscattered fields were directly related to the load at the port of the RFID antenna. The Friis transmission line equation was used to clearly show what determines the max read range of a passive RFID tag. The discussion on antenna apertures revealed how in the best possible situation only half of the incident power from the reader can be used by the passive IC. The rest of the power is scattered into the region around the tag. Next, a design methodology for producing compact space-filling antennas was presented. This section was immediately followed by two examples showing this design process. The result of this chapter is an understanding of the fundamental and important concepts of RFID systems and a structured design process for producing compact, useful space-filling antennas for many different applications.

7. References

- Advanced Design System, Agilent Technologies, www.agilent.com.
- Amin, Y.; Batao, S.; Hallstedt, J.; Prokkola, S.; Tenhunen, H.; & Zhen, L.-R., "Design and characterization of efficient flexible UHF RFID tag antennas," *3rd European Conference on Antennas and Propagation*, pp. 2784-2786, March, 2009, Berlin, Germany.
- Balanis, C.A. (2005). *Antenna Theory: Analysis and Design*, 3rd ed., Harper and Row, Publishers, New York.
- Braaten, B.D.; Feng, Y. & Nelson, R.M., "High-frequency RFID tags: an analytical and numerical approach for determining the induced currents and scattered fields," *IEEE International Symposium on Electromagnetic Compatibility*, pp. 58-62, August 2006, Portland, OR.
- Braaten, B. D.; Owen, G. J.; Vaselaar, D.; Nelson, R. M.; Bauer-Reich, C.; Glower, J.; Morlock, B; Reich, M.; & Reinholz, A., "A printed Rampart-line antenna with a dielectric superstrate for UHF RFID applications," in *Proceedings of the IEEE International Conference on RFID*, pp. 74-80, April, 2008, Las Vegas, NV.
- Braaten, B. D.; Scheeler, R. P.; Reich, M.; Nelson, R. M.; Bauer-Reich, C.; Glower, J. & Owen, G. J., "Compact metamaterial-based UHF RFID antennas: deformed omega and split-ring resonator structures," *Accepted for publication in the ACES Special Journal Issue on Computational and Experimental Techniques for RFID Systems and Applications*, 2009.

- Calabrese, C. & Marrocco, G., "Meander-slot antennas for sensor-RFID tags," *IEEE Antennas and Wireless Propagation Letters.*, vol. 7, pp. 5-8, 2008.
- Cooney, E. (2005). *RFID+:The Complete Review of Radio Frequency Identification*, Cengage Delmar Learning.
- Curty, J.-P.; Declercq, M.; Dehollain C. & and Joehl, N. (2006). *Design and Optimization of Passive UHF RFID Systems*, Springer-Verlag New York, LLC.
- Eleftheriates, G. V. & Balmain, K. G. (2005) *Negative-Refraction Metamaterials: Fundamentals Principles and Applications*, John Wiley and Sons, Hoboken, New Jersey.
- Feng, Y.; Braaten, B.D. & Nelson, R.M., "Analytical expressions for small loop antennas-with application to EMC and RFID systems," *IEEE International Symposium on Electromagnetic Compatibility*, pp. 63-68, August 2006, Portland, OR.
- Finkenzeller, K. (2003). *RFID Handbook:Fundamentals and Applications in Contactless Smart Cards and Identification*, John Wiley and Sons, West Sussex, England.
- Hunt, V.D.; Puglia, A. & Puglia, M. (2007). *RFID-A Guide to Radio Frequency Identification*, John Wiley and Sons, Inc.
- Lee, C.-J.; Leong, K. M. K. H. & Itoh, T, "Design of a resonant small antenna using composite right/left-handed transmission line," *IEEE Antennas and Propagation Society International Symposium*, July, 2005, Washington, DC.
- Lee, C.-J.; Leong, K. M. K. H. & Itoh, T, "Composite right/left-handed transmission line based compact resonant antennas for RF module integration," *IEEE Transactions on Antennas and Propagation*, vol. 54, no. 8, August, 2006, pp. 2283-2291.
- Li, H.-J.; Lin, H.-H. & Wu, H.-H., "Effect of antenna mutual coupling on the UHF passive RFID tag detection," *IEEE Antennas and Propagation Society International Symposium*, July, 2008, San Diego, CA.
- Mao, S.-G.; Chueh Y.-Z. & Wu, M.-S., "Asymmetric dual-passband coplanar waveguide filters using periodic composite right/left-handed and quarter-wavelength stubs," *IEEE Microwave and Wireless Components Letters*, vol. 17, no. 6, June, 2007, pp. 418-420.
- Marques, R.; Martin, F. & Sorolla, M. (2008). *Metamaterials with Negative Parameters: Theory, Design and Microwave Applications*, John Wiley and Sons, Inc., Hoboken, New Jersey.
- Mirza, I.O.; Shi, S.; Fazi, C.; and Prather, D. W., "Stacked patch antenna miniaturization using metamaterials," *IEEE Antennas and Propagation Society International Symposium*, July, 2008, San Diego, CA.
- Owen, G. J.; Braaten, B. D.; Nelson, R. M.; Vaselaar, D.; Bauer-Reich, C.; Glower, J.; Reich, M.; & Reinholz, A., "On the Effect of Mutual Coupling on LF and UHF Tags Implemented in Dual Frequency RFID Applications," *Proceedings of the 2009 IEEE International Symposium on Antennas and Propagation*, June, 2009, Charleston, SC.
- Paret, D.; Riesco R.; & Riesco, R. (2005). *RFID and Contactless Smart Card Applications*, John Wiley and Sons, Inc..
- Qing, X. & Chen, Z.N., "Proximity effects of metallic environments on high frequency RFID reader antenna: Study and Applications," *IEEE Transactions on Antennas and Propagation*, vol. 55, no. 11, November, 2007, pp. 3105-3111.
- Rao, K. V. S.; Nikitin, P.V.; & Lam, S.F., "Antenna Design for UHF RFID Tags: A Review and a Practical Application," *IEEE Transactions on Antennas and Propagation*, vol. 53, no. 12, December, 2005, pp. 3870-3876.

- Sanford, J. R., "A novel RFID reader antenna for extreme environments," *Proceedings of the IEEE International Symposium on Antennas and Propagation*, July, 2008, San Diego, CA.
- Stutzman, W.L. & Thiele, G.A. (1998). *Antenna Theory and Design*, 2nd ed., John Wiley and Sons, Inc., New York.
- Yen, C.-C.; Gutierrez, A.E.; Veeramani, D.; & Van der Weide, D., "Radar Cross-Section Analysis for Backscattering RFID Tags," *IEEE Antennas and Wireless Propagation Letters*, vol. 6, 2007, pp. 279-281.
- Ziolkowski, R. W. & Lin, C.-C., "Metamaterial-inspired magnetic-based UHF and VHF antennas," *IEEE Antennas and Propagation Society International Symposium*, July, 2008, San Diego, CA.